EUROPEAN
COMMISSION
European
Research Area

CArbon-14 Source Term

CAST

Annual progress report on corrosion test (D3.10)

Author(s):

Viktor Jobbágy (SCK•CEN), Frank Druyts (SCK•CEN), Tomofumi Sakuragi (RWMC),
Manuela Fulger (RATEN ICN), Crina Bucur (RATEN ICN), David Bottomley (JRC-ITU)

Date of issue of this report: 12/11/2015

The project has received funding from the European Union’s European Atomic Energy Community’s (Euratom) Seventh Framework Programme FP7/2007-2013 under grant agreement no. 604779, the CAST project.		
Dissemination Level		
PU	Public	x
RE	Restricted to the partners of the CAST project	
CO	Confidential, only for specific distribution list defined on this document	

EURATOM

CAST – Project Overview

The CAST project (CArbon-14 Source Term) aims to develop understanding of the potential release mechanisms of carbon-14 from radioactive waste materials under conditions relevant to waste packaging and disposal to underground geological disposal facilities. The project focuses on the release of carbon-14 as dissolved and gaseous species from irradiated metals (steels, Zircaloys), irradiated graphite and from ion-exchange materials.

The CAST consortium brings together 33 partners with a range of skills and competencies in the management of radioactive wastes containing carbon-14, geological disposal research, safety case development and experimental work on gas generation. The consortium consists of national waste management organisations, research institutes, universities and commercial organisations.

The objectives of the CAST project are to gain new scientific understanding of the rate of release of carbon-14 from the corrosion of irradiated steels and Zircaloys and from the leaching of ion-exchange resins and irradiated graphites under geological disposal conditions, its speciation and how these relate to carbon-14 inventory and aqueous conditions. These results will be evaluated in the context of national safety assessments and disseminated to interested stakeholders. The new understanding should be of relevance to national safety assessment stakeholders and will also provide an opportunity for training for early career researchers.

For more information, please visit the CAST website at:
http://www.projectcast.eu

CAST		
Work Package: 3	CAST Document no. :	Document type:
Task: 3.3	CAST-2015-D3.10	R = report
Issued by: SCK.CEN		Document status:
Internal no. : not applicable		Final

Document title
Annual progress report on corrosion tests

Executive Summary

This document gives an overview of progress on the Zircaloy corrosion activities performed or planned in Work Package 3. Five project partners (INR, JRC-ITU, KIT, RWMC and SCK•CEN) gave details on the progress in this task.

RATEN ICN established both corrosion rates and mass loss rates ‘measurements for unirradiated Zry-4. It was found that oxidized samples had the lowest corrosion rates and mass loss rates, and the presence of oxygen (aerobic or anaerobic conditions) had no influence on the corrosion rates. Additionally, the oxide layer thickness of unirradiated Zry-4 was measured by optical microscopy.

JRC-ITU described the experimental plan related to the corrosion tests, where Zircaloy-4 will be used. Different cleaning procedures will be used depending on the origin and the contamination of the samples. The corrosion rates determination will be based on Co-60 (gamma-spec) measurement.

The progress at KIT was already detailed in D3.8. Therefore, achievements were not reported in this report.

RWMC performed two different experiments to determine the corrosion rate of unirradiated Zircaloys: 1) Continuous hydrogen measurement for unirradiated materials by gas flow method and 2) Hydrogen measurement for unirradiated materials by glass ampoule method tests in a glove box. An experiment was conducted to determine the corrosion rate for irradiated Zircaloy-2 material.

SCK•CEN has made minor modifications on the experimental setup of the electrochemical cell devoted to corrosion rate measurements. They concern the electrolyte, compartment and test cell lining. The glass cells were proved to be gas tight on the course of a test with helium. Experiments on unirradiated materials are expected to start by the end of 2015.

List of Contents

1 Work in progress at KIT

The progress made in the second year with the corrosion experiments at KIT is presented in a separate report (Deliverable 3.8 (Herm et al., 2015)). For details and achievements the referred document should be consulted.

2 Work in progress at RWMC

2.1 *Corrosion rate of zirconium materials*

2.1.1 Continuous hydrogen measurement for unirradiated materials by gas flow method

Zircaloy-4 and Zircaloy-2 were obtained from CEZUS Co., Ltd. The samples were pre-treated to produce an appropriate thickness by undergoing two sets of cold-rolling, followed by vacuum annealing after each set to remove the hydrogen absorbed during cold-rolling. The final polishing was done with 0.02 mm alumina powder. The initial hydrogen content was measured and found to be lower than 10 ppm. Zircaloy foils (100 sheets: 100 mm×100 mm×0.1 mm, surface area of 2.0 m^2) were immersed in a dilute NaOH solution (~0.03 M, pH 12.5) kept at 303 K (see Figure 1). Argon carrier gas with oxygen concentration below 1×10^{-3} ppm was passed through the glass flask at a flow rate of 0.9 dm^3/min, and the hydrogen concentration in the carrier gas was measured periodically by using atmospheric pressure ionization mass spectrometry (API-MS). Zircaloy coupons (20 mm×30 mm×0.05 mm) in a separate flask under similar condition were collected after immersion, and the absorbed hydrogen content was determined by an inert gas melting system together with gas chromatography (LECO RH-404).

The following corrosion reaction was assumed for hydrogen absorption ratio x:

$$(2x+1)\mathrm{Zr}+2\mathrm{H_2O}\rightarrow \mathrm{ZrO_2}+2\mathrm{x}\cdot\mathrm{ZrH_2}+2(1-\mathrm{x})\mathrm{H_2} \qquad (1)$$

The cumulative atomic molar amount of gaseous hydrogen per surface area unit, A_{gas} (mol/m^2), and the molar amount of hydrogen absorbed in Zircaloy metal per surface area unit, A_{abs} (mol/m^2), were obtained. In the gas flow method, the corrosion rate, R_c (µm/y), which represents the amount of zirconium consumed by oxidation and hydriding under stoichiometry in equation (2), can be obtained from:

$$R_c = \frac{(2x+1)\cdot A_{gas}\cdot M_{Zr}\cdot 10^6}{4(1-x)\cdot \rho \cdot t}\,. \qquad (2)$$

where M_{Zr} is the molecular weight of zirconium (91.22 g/mol), ρ is the zirconium density (6.44×10^6 g/m^3), t is test time, and x represents the hydrogen absorption ratio $x = A_{abs}/(A_{gas}+A_{abs})$. Here, hydrogen absorption can be assumed constant during experiment with values of 91% for Zircaloy-4 and 94% for Zircaloy-2 (see Table 1).

Details for the gas flow experiment were described by Sakuragi et al. (2013).

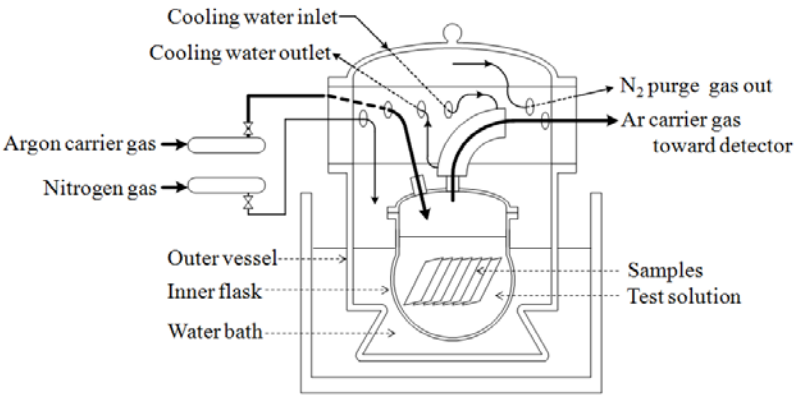

Figure 1: Test vessel for the gas flow experiment.

Table 1 Hydrogen gas generation and absorption obtained from the gas flow experiment (T.Sakuragi, H.Miyakawa et al. 2013).

Material	Day	A_{gas} (mol/m^2)		A_{abs} (mol/m^2)		x (%)
		Run 1	Run 2	Coupon 1	Coupon 2	
Zircaloy -4	1	6.18×10^{-6}	3.69×10^{-6}	-	-	-
	10	1.89×10^{-5}	1.94×10^{-5}	-	-	-
	30	2.95×10^{-5}	3.08×10^{-5}	1.85×10^{-4}	1.92×10^{-4}	86
	90	-	4.96×10^{-5}	5.53×10^{-4}	4.64×10^{-4}	91
	180	7.11×10^{-5}	6.69×10^{-5}	7.86×10^{-4}	7.04×10^{-4}	92
	365	9.71×10^{-5}	9.01×10^{-5}	1.14×10^{-3}	1.26×10^{-3}	93
	730	1.45×10^{-4}	1.36×10^{-4}	1.44×10^{-3}	1.74×10^{-3}	92
	1000	1.71×10^{-4}	1.63×10^{-4}			(Average 91%)
	1500	2.16×10^{-4}	2.10×10^{-4}			
Zircaloy -2	1	3.39×10^{-6}	-	-		-
	10	1.39×10^{-5}	-	-		-
	30	2.26×10^{-5}	-	1.65×10^{-4}	3.04×10^{-4}	92
	90	3.66×10^{-5}	-	4.94×10^{-4}	7.23×10^{-4}	94
	180	5.07×10^{-5}	-	9.34×10^{-4}	7.90×10^{-4}	94
	365	7.60×10^{-5}	-	1.26×10^{-3}	1.41×10^{-3}	95
	730	1.18×10^{-4}	-	1.68×10^{-3}	1.95×10^{-3}	94
	1000	1.42×10^{-4}	-			(Average 94%)

2.1.2 Hydrogen measurement for unirradiated materials by glass ampoule method

Specimens were prepared as described in 2.1.1. 23 Zircaloy strips (21 pieces; 3 mm×90 mm×0.1 mm, 2 pieces; 3 mm×90 mm×0.05 mm) were placed in a glass ampoule. The outline for test procedure is shown in Figure 2. A stop-cock was attached, then the ampoule was filled with NaOH solution (pH 12.5) and the stop-cock closed. This enclosure procedure was performed in a glove box that had been purged by nitrogen gas with oxygen concentration below 0.1 ppm. The ampoules were moved outside the glove box and sealed by heating. After corrosion, the ampoules were set on the vacuum gas collecting system connected with a gas chromatography (YANACO G-2800) and hydrogen gas was measured. The hydrogen absorbed into the metal was also measured by an inert gas melting system together with gas chromatography (LECO RH-404).

In the ampoule method, the corrosion rate, R_c (μm/y), is obtained from the following equation (3) based on the oxidation and hydriding reaction under stoichiometry in equation (3).

$$R_c = \frac{(A_{gas} + 3 \cdot A_{abs}) \cdot M_{Zr}}{4 \cdot \rho \cdot t} \cdot 10^6 \qquad (3)$$

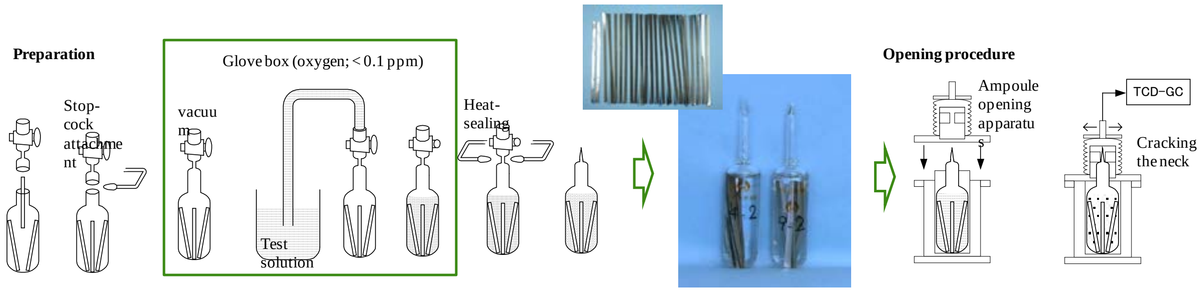

Figure 2: **Procedure for ampoule batch corrosion experiment.**

2.1.3 Irradiated Zircaloy-2

Irradiated Zircaloy-2 claddings (STEP I and STEP III types) from a BWR were prepared. Here, STEP I is an older fuel type in Japan (Lattice configuration of 8×8 array, average burnup of 33 GWd/t) and STEP III is relatively new fuel type (Lattice configuration of 9×9 array, average burnup of 45 GWd/t). (Ken'ichi Ito, Katsumasa Haikawa et al. 1998). The claddings were cut to heights of 2 cm for the leaching tests. The bonding fuel elements were removed by mechanical polishing and washed with 4 M boiling nitric acid for 4 hours. The oxide films were also removed by polishing the surfaces. A part of the cladding was used to measure the nuclides inventory.

The leaching tests were performed in a dilute NaOH solution of pH 12.5 and nitrogen atmosphere at room temperature using a glass vial with a gastight outer vessel as shown in Figure 3. After immersion, C-14 in gas phase was collected using a plastic bag. Leached radionuclides and Zircaloy additive elements in solution were measured by LSC, gamma spectrometry and ICP-MS.

Assuming that the activated radionuclides and additive elements are distributed homogeneously in the cladding, the equivalent corrosion rate, R_{eq} (μm/y), can be obtained from leachates as (4):

$$R_{eq} = \frac{aL}{2At} \tag{4}$$

Where, *a* is the leached amount of radionuclides or elements (Bq or mol), *A* is the inventory in the cladding (Bq or mol), *L* is the thickness of the cladding (μm), and *t* is the test time (years). Namely, the leaching fraction is represented as *a/A*. Here, the thickness *L* is 740 μm based on the cross-sectional optical microscopy for STEP I cladding.

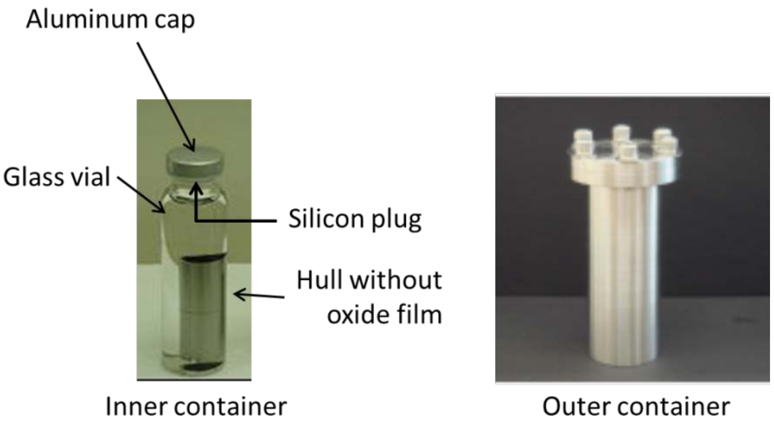

Figure 3: **Test vessels for irradiated cladding.**

2.2 *Test results*

The results of corrosion rate are shown in Figure 4. The data for gas flow experiments are obtained from Sakuragi et al. (2013). A part of the ampoule test (Kato et al., 2014) and

BWR data (Yamashita, et al., 2014) can be found in the literature. The PWR data are obtained from the work of Yamaguchi et al. (1999).

In the hydrogen measurements from unirradiated Zircaloy, the corrosion rate decreases with time. Detailed analysis of the gas flow experiment data has found that the corrosion kinetics are represented by the parabolic rate law (Sakuragi, et al., 2013). This kinetic result differs from the general out-pile (high temperature) corrosion behavior of the cubic rate law. The corrosion rate increases as the temperature increases. The difference between Zircaloy-2 and Zircaloy-4 is negligible. In comparison with the case of pure water it is possible that the solution components and increased pH slightly enhance the corrosion rate.

The equivalent corrosion rates for irradiated cladding are somewhat complicated. The extremely low values for zirconium are probably due to the low solubility of zirconia (oxide film). The other elements and radionuclides might be incorporated in the oxide film. The congruence of C-14 leaching with the corrosion rate of Zr cannot be confirmed yet. However, it should be noted that the corrosion rate obtained by hydrogen measurement, which takes into account both, oxidation and hydride formation from anodic dissolution of zirconium (equation 1), is affected by hydrogen absorption ratio (x). According to equation (2), the corrosion rate at hydrogen absorption ratio of 100% is 3 times larger than that without hydriding. The hydriding effect is not clearly presented in Figure 4.

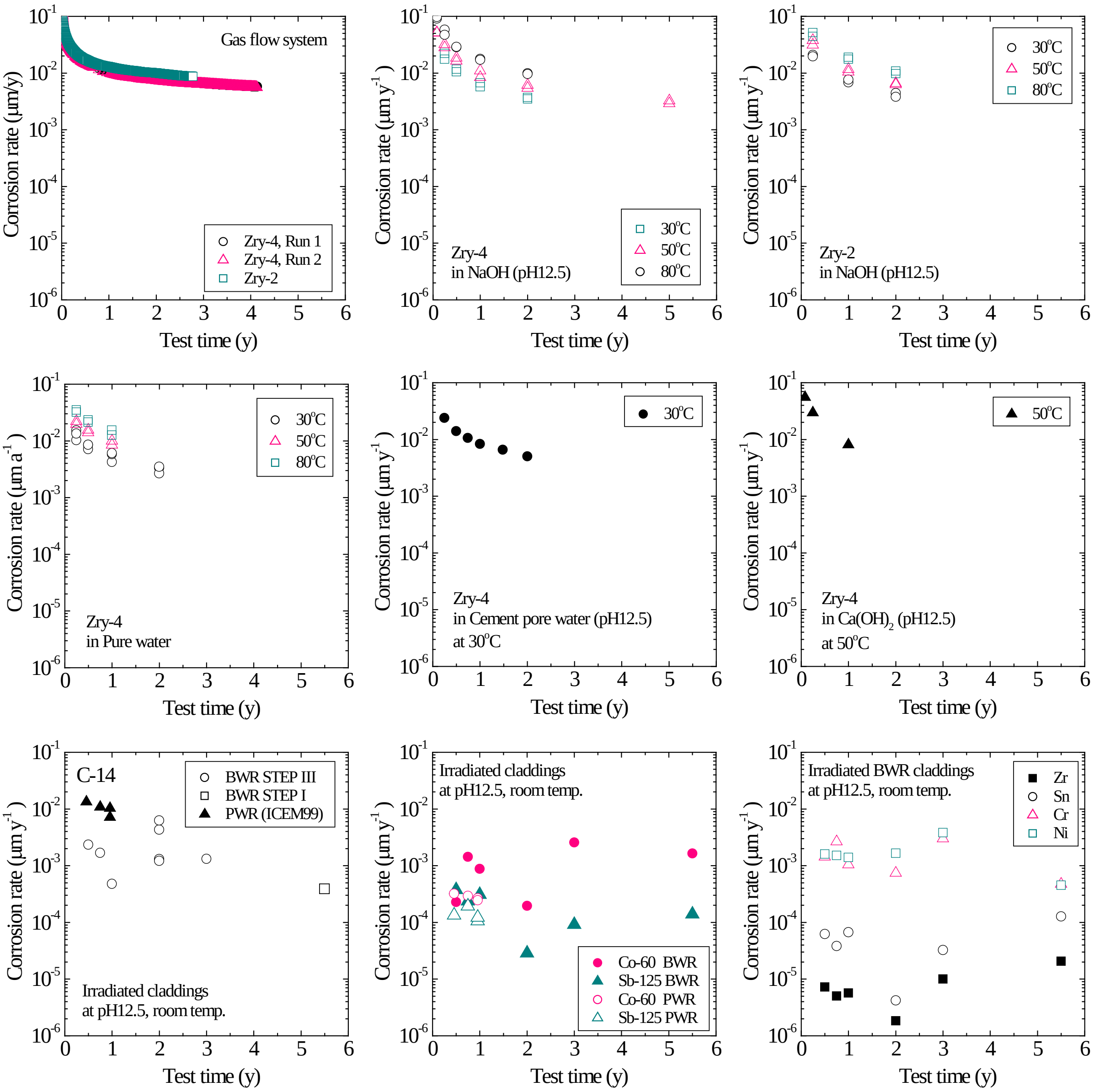

Figure 4: **Corrosion rate for zirconium materials.**

2.3 *Acknowledgement*

This research is a part of the “Research and development of processing and disposal technique for TRU waste (FY2014)” program funded by Agency for Natural Resources and Energy, Ministry of Economy, Trade and Industry of Japan.

3 Work in progress at SCK.CEN

3.1 *Introduction*

Static leaching and electrochemical (LPR) tests are planned for non-irradiated and irradiated samples. In the WP2 and WP3 technical meeting in Switzerland (27-28 May 2015), a solution of NaOH at pH 12 at room temperature, was recommended to run the leaching test. However, each participant is allowed to use its own electrolyte. For this reason SCK•CEN reconsidered the original approach and decided to continue its experiments using $Ca(OH)_2$ electrolyte. The main reason is that portlandite is representative to the Belgian national nuclear waste repository situation. The following pore water is planned to be used for the leaching/corrosion tests: de-gassed $Ca(OH)_2$ (pH ~12.5). The pore water will be prepared in a glove box under anaerobic conditions and degassed with (nitrogen or argon) to reduce the risk of any traces of environmental origin $^{14}CO_2$ absorbed in the solution. The risk of calcite precipitation cannot be excluded as described by the calculations (Report D3.5) (S.Necib, Bottomley et al. 2014).

After consulting with the SCK•CEN`s radiation protection officers on the dose exposure and the associated risks, it was concluded that the experiments can be carried out in glove box and fume hoods using plastic glove bags. Hot cells at SCK•CEN may not be available within a reasonable timeframe which is another reason why glove box or glove bag is preferred.

3.2 *Materials*

Non-irradiated and irradiated Zircaloy samples (Zircaloy-2/4 and M5™ (current reference cladding for AREVA fuel) will be studied. AREVA needs to provide an authorisation to SCK.CEN to work on M5™ material. A request was sent to AREVA in August 2014 but approval is still pending as their official response has not yet been received. Therefore, it was decided to work on irradiated Zy-4 only.

3.2.1 Nitrogen content

Information on the nitrogen content from recent experimental studies and reports were either not available or not presented accurately (i.e. only maximum permitted values).

Therefore, the initial nitrogen content within the metals was desirable to realistically estimate the ^{14}C production after irradiation campaigns.

The nitrogen contents of Zircaloy-4 samples were measured by using an inert gas fusion method. The nitrogen content measurements were performed by using a LECO TC436 model analyser. The sample was placed inside a graphite crucible and held between the upper and lower electrodes of impulse furnace. A high current passed through the crucible, enhancing an increase of the inner temperature (> 2500 ºC), and leading eventually to the melting of the sample. Gaseous compounds generated in the furnace were released into a flowing inert gas stream (argon or helium). The gas stream was sent to the appropriate infrared detector. If O as CO_2 is measured, then the thermal conductivity detector detects nitrogen. The reported lower limit of detection of the method is approximately 1 ppm for N. Results are presented in Table 2.

Table 2 Average nitrogen content (Navg) of unirradiated Zircaloy samples.

Sample ID	**material**	**N_{avg} (ppm)**
ZR4 19430	Zircaloy-4	17 ± 3.9
ZR4 M92029	Zircaloy-4	25 ± 2.6

It can be concluded that the nitrogen content of Zircaloy-4 is lower than the values given in the literature and technical specifications (usually between 40-80 ppm). The M5^{TM} sample will be analysed after approval from AREVA.

3.2.2 Metallography

Metallography was carried out on unirradiated metals after the appropriate sample treatment (W.Van-Renterghem 2015).

The transmission electron microscopy (TEM) investigation was conducted in a JEOL 3010 microscope operating at 300 kV. Bright field, dark field and selected area electron diffraction were used to determine the defect structure and precipitates. Energy dispersive

X-ray spectroscopy (EDS) was carried out for the qualitative determination of the composition of the precipitates. The grain size of each material was determined from the backscattered electron images (BEC) of the samples after electrochemical polishing for 10 seconds in a solution of 5% perchloric acid and 95% methanol. The grain size is determined in accordance with the ASTM standard E112-95(ASTM 2013). Figure 5 presents the BEC image of a Zry-4 samples as well as the EDS analyses conducted on a precipitate and the bulk.

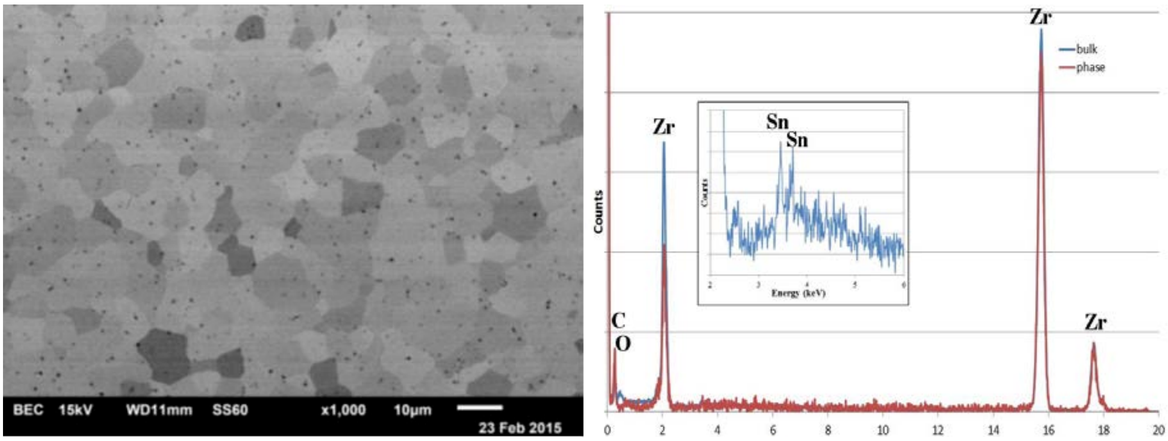

Figure 5 Backscattered electron images of a Zry-4 sample (left); EDS spectrum (right).

This Zry-4 material consists of small uniform equiaxed grains. The grain size number determined from the SEM images is 11.8, which corresponds to an average grain surface of 36.4 µm² or a grain diameter of 6 µm. The small black spots can be attributed to the Laves phases.

The EDS spectrum in Figure 5 shows the composition of the precipitate in comparison to the spectrum of the bulk Zry4. According to the spectrum of the precipitate, only Zr and C are detected. In addition, the carbon content is significantly higher than in the spectrum of the bulk material. The EDS results together with the crystal structure analysis confirmed the presence of carbides as ZrC precipitates.

The analysis of the irradiated samples will be made at the end of 2015.

3.3 Linear polarization resistance (LPR) test

Special glassware and electrodes have been designed for the LPR setup. The inner part of the glass cell will be covered with a PEEK liner to avoid interference due to glass dissolution at high pH.

Preliminary gas tightness tests have been conducted on the cell. Rubber sealing was used between the cell-lid and the cell vessel. The cell was filled with helium and the internal and ambient air pressure was together with the ambient temperature were recorded. Pressure in the glass cell was set to 1.1 bar, that is 0.1 bar overpressure comparing to the ambient pressure. Therefore, air entrance will be avoided. The glass cell for the LPR experiment is shown in Figure 6. The stability of the gas pressure is demonstrated in Figure 7. The updated experimental layout is shown in Figure 8.

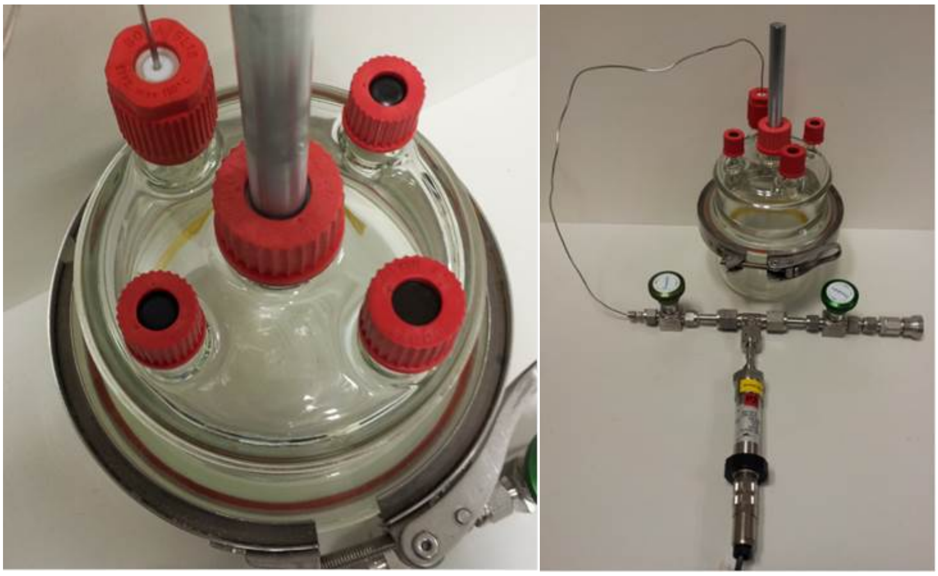

Figure 6: Glass cell for LPR test setup.

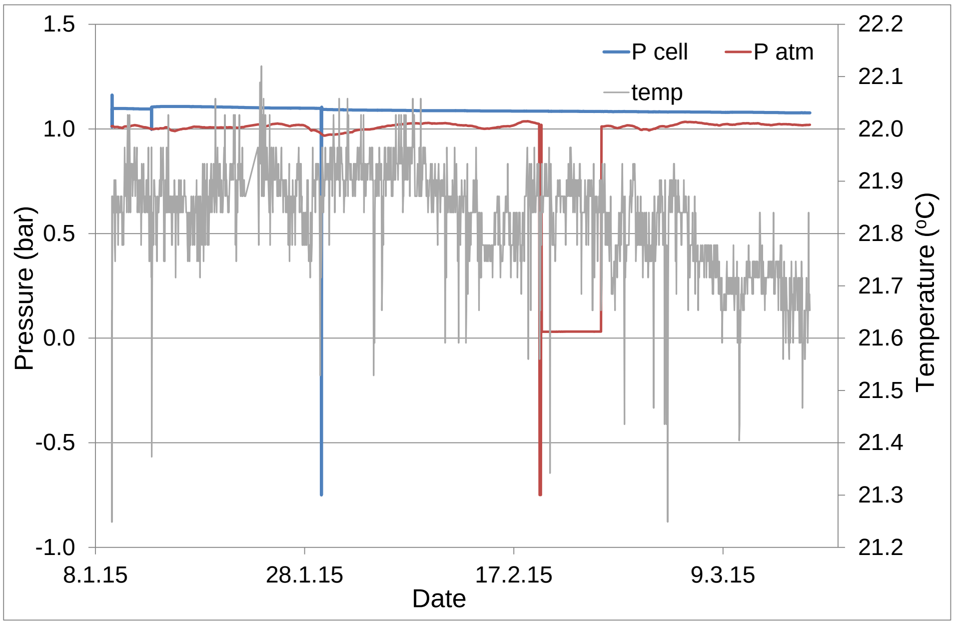

Figure 7: Temperature, internal- and external pressure profile during the gas tightness test.

The sharp decreases in the temperature and pressure indicate interruptions or replacement of the sensors.

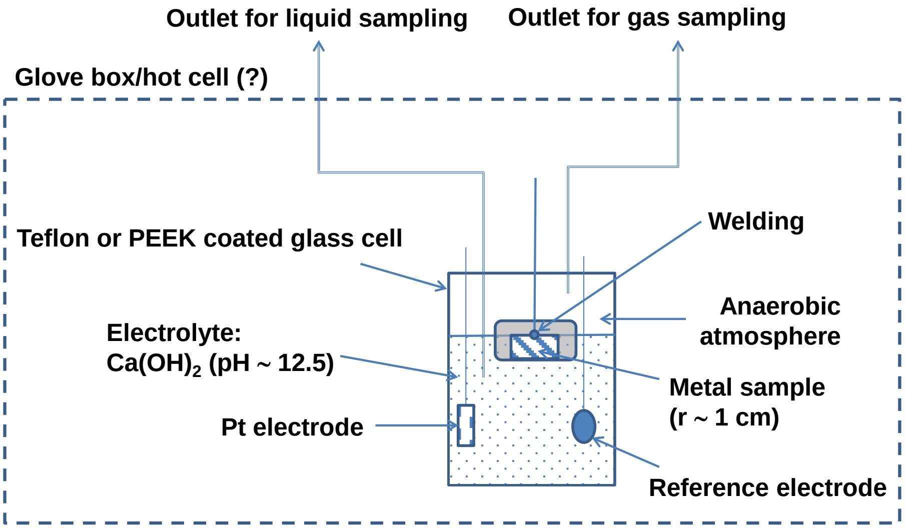

Figure 8: The updated layout of the LPR test setup in glove box/glove bag under reducing atmosphere.

4 Work in progress at RATEN ICN

4.1 *Electrochemical tests on un-irradiated Zircaloy-4 in NaOH solution at pH12*

In the first part of the second year, the experiments consisted of electrochemical tests on un-irradiated Zy-4 samples to establish a working procedure for testing irradiated Zy-4 samples. The samples were cut from as-received Zy-4 tube with OD of 13 mm and wall thickness of 0.4 mm.

Initially, the un-irradiated Zy-4 samples were oxidised in autoclaves to obtain a similar oxide film as spent Zy-4 claddings. An oxide thickness above 2.5 µm was required for the project.

The tests were conducted in static isothermal autoclaves in similar conditions to a CANDU primary circuit (LiOH solution, pH=10.5, T=310 ^{o}C, p=100 atm). After 172 days in the autoclaves, the average weight gain of Zr samples was 29.3 mg/dm^2. The weight gain of the corroded specimens can be used as a direct gauge of the oxide film thickness, taking into account that 14.9 mg/dm^2 of Zr oxide represents 1µm thickness. In the case of these samples, the thickness was 1.96 µm corresponding to a weight gain of 29.3 mg/dm^2**.** The thickness of the oxides after 172 days of exposure in autoclaves was also measured by optical microscopy and estimated to be in the range of 1.7-2.2 µm (see Figure 9).

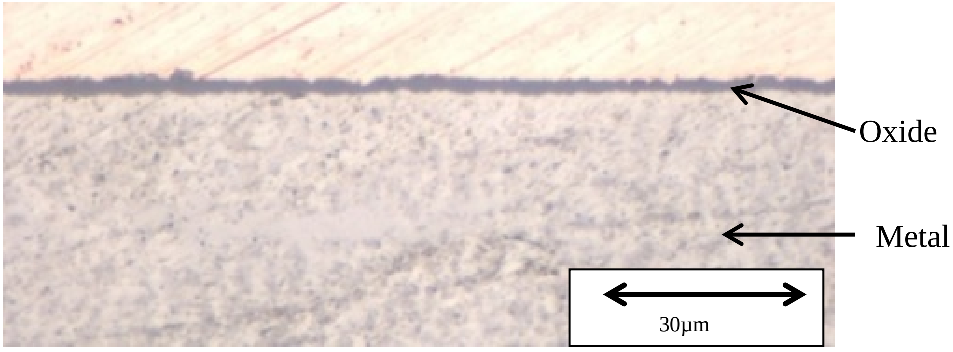

Figure 9: Oxide layer thickness measured by optical microscopy (magnification x1000).

Hydrides present in Zy-4 tubes, were also determined by optical microscopy. The materials were Zy-4 tubes oxidized in simulated conditions of CANDU primary circuit (Figure 10).

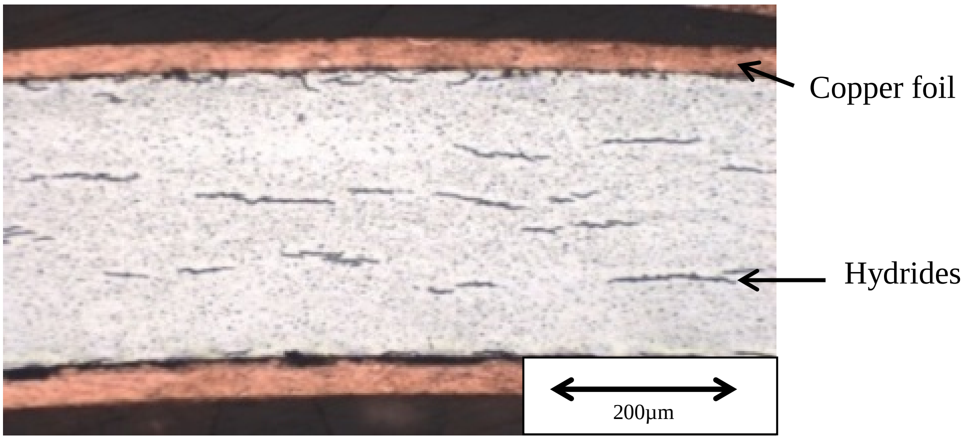

Figure 10 Hydrides in Zy-4 tubes after 172 days of oxidation (optical microscopy x100).

4.2 *Electrochemical set-up*

The device used for electrochemical tests was a potentiostat/galvanostat AUTOLAB 302 electrical connected to a corrosion glass (borosilicate glass) cell equipped with a Pt counter electrode and a Ag/AgCl reference electrode. The software used was NOVA 11.1. The three electrode electrochemical cell was filled with a 50 ml solution of NaOH (0.01 M) at pH=12 with a conductivity of 2.1 mS/cm. The working electrode was simply immersed into the electrolyte and electrically connected to the potentiostat. Corrosion tests have only been performed at room temperature. Argon was bubbled for 2 hours before testing and throughout the duration of the test. All the electrodes and the gas bubbling tube were introduced through a vessel lid with 5 openings and were made gas-tight by adding resin or glue around them. The electrochemical assembly was mounted into a Faraday cage during tests to protect the set up against electromagnetic interference from external sources (Figure 11).

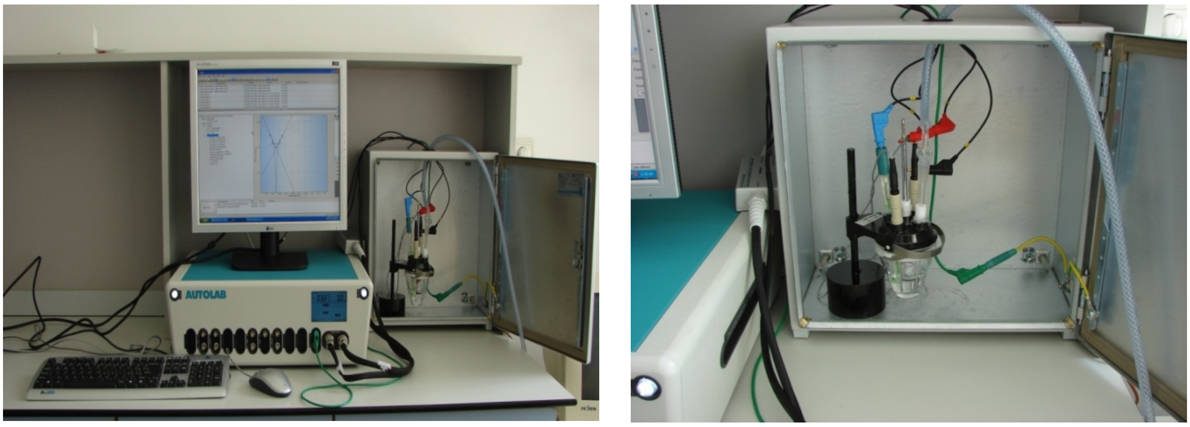

Figure 11: Electrochemical set-up.

The Linear Polarization Resistance measurement have been performed by scanning through a potential range very close to the free corrosion potential E_{corr}. At the begining of the test the sample is kept for 10 minutes in simple contact with the solution (without electrical connection) to stabilise $E_{corr.}$ The potential imposed was in the range of ± 25 mV around E_{corr} with a scan rate of 0.16mV/sec. After testing, the NOVA software provides a convenient interface for making Tafel plots, calculating Tafel slopes and corrosion rates.

Selecting corrosion rate fit, the analysis tool performs a curve fit based on the Buttler-Volmer equation which allows for more accurate determination of the corrosion current density (i_{corr}), polarisation resistance (Rp) and corrosion rate. Calculation of corrosion rates requires the determination of corrosion currents. When reaction the mechanism for the corrosion reactions is known, the corrosion currents can be calculated by using Tafel slope analysis. The relationship between the current density and potential of anodic and cathodic reactions under charge transfer control is given by the Buttler -Volmer equation:

$$i = i_{corr}\left(e^{2.303\eta/ba} - e^{2.303\eta/bc} \right) \qquad (5)$$

Where:

$\eta = E - E_{corr}$ (overpotential)
E = applied potential (V)
E_{corr}= corrosion potential (also called open circuit potential)(V)

i = measured current density(A/cm^2)

i_{corr}= corrosion current density (A/cm^2)

ba, bc = Tafel constants

The corrosion curent density may be calculated from the polarization resistance and Stern-Geary constant as follows:

$i_{corr}= B/R_p$ (6)

Where:

B= Stern-Geary constant (V)

Rp = polarization resistance(Ω)

4.3 Results from LPR method

LPR tests have been performed on the following samples (see Figure 12):

- As received Zy-4 tube (aerobic condition),
- As received Zy-4 tube (anaerobic condition),
- Oxidised Zy-4 tube (aerobic condition),
- Oxidised Zy-4 tube (anaerobic condition),
- Oxidised Zy-4 tube cut at the end (aerobic condition),
- Oxidised Zy-4 tube cut and painted (aerobic condition).

Figure 12. Oxidised Zy-4 tube uncut (left), oxidised Zy-4 tube cut at the end (middle) and oxidised Zy-4 tube cut and painted (right).

The last two samples were tested because to also consider the situation of coupons cut from spent Zy-4 claddings when the end cut is fresh metal exposed in solution. The immersed surface of the samples was ~ 2.5cm^2. The Tafel plots are presented in Figure 13and the electrochemical parameters calculated from the Tafel plots, are presented in Table 3.

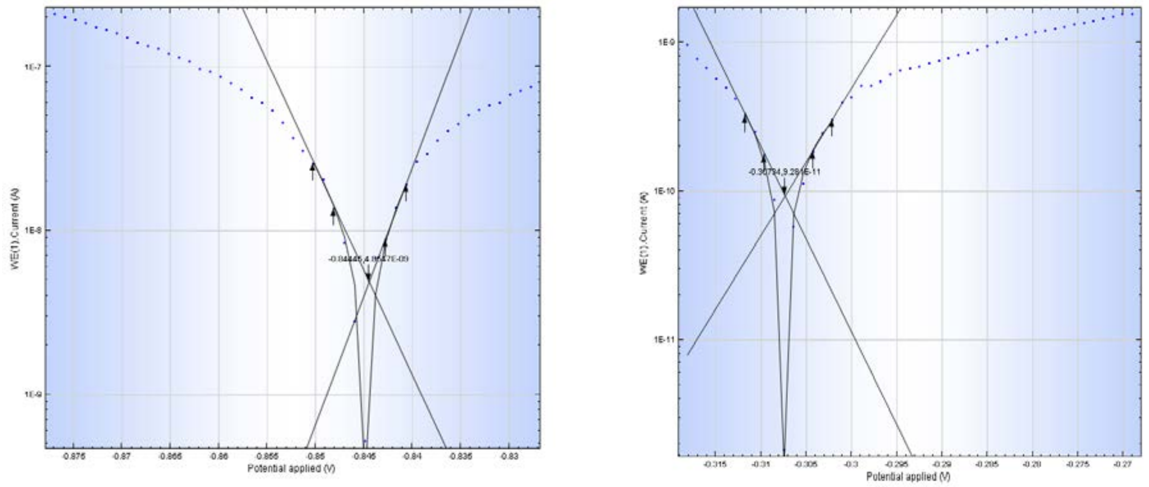

Figure 13: Example of Tafel plots for two tested samples

Table 3: Electrochemical parameters calculated from Tafel plots.

Samples	ba (V/dec)	bc (V/dec)	Ecorr (V)	icorr (A/cm²)	Corr rate (mm/y)	Rp (Ω)	E begin (V)	E End (V)
As received Zy-4 tube (aerobic condition)	0.03	0.03	-0.52	4.1E-8	4.8E-4	1.4E+5	-0.53	-0.52
As received Zy-4 tube (anaerobic condition)	0.01	0.01	-0.84	1.0E-8	1.1E-4	2.4E+5	-0.85	-0.84
Oxidised Zy-4 tube (aerobic condition)	0.07	0.11	-0.13	8.8E-10	9.7E-6	5.4E+6	-0.13	-0.12
Oxidised Zy-4 tube (anaerobic condition)	0.03	0.20	-0.30	2.7E-10	3.1E-6	1.5E+7	-0.31	-0.32
Oxidised Zy-4 tube cut (aerobic condition)	0.05	0.33	-0.40	1.0E-9	1.1E-5	2.0E+7	-0.41	-0.39
Oxidised Zy-4 tube cut and painted (aerobic condition)	0.01	0.03	-0.40	3.1E-10	3.6E-6	1.3E+7	-0.40	-0.40

The conversion of electrochemical corrosion rates to mass loss rate was done by using the ASTM G 102-2004 standard. The determination of i_{corr} over a known period of time leads to the direct determination of the mass loss. Faraday's law can be used to calculate the corrosion rate, either in terms of penetration rate (CR) (Equation (7)) or mass loss rate (MR) (Equation (8)).

$$CR = K_1 (i_{corr}/\rho) E_W \qquad (7)$$

Where:

CR=penetration rate (nm/y)

K_1= 3.27x10^{-3}, (mm g/µA cm y)

i_{corr} = corrosion density current (µA/cm^2)

ρ = density (g/cm^3)

E_W = equivalent weight (is not dependent on the unit system chosen so may be considered dimensionless) E_W = 22.8 (Atomic mass Zr / (number of exchanged electrons))

$$MR= K_2 i_{corr} E_W \qquad (8)$$

Where:

- MR = mass loss rate (mg/dm^2d)
- K_2 = 0.0895 mgcm^2/µAdm^2d

The calculation of penetration or mass loss rate from electrochemical measurements, as described in ASTM 102-2004, assumes that uniform corrosion is occurring.

InTable 4, the corrosion rates and mass loss rates are presented for unirradiated Zy-4 after LPR measurements. Oxidized samples had the smallest corrosion rates and mass loss rates, and the aerobic or anaerobic conditions had no influence on the corrosion rates.

Table 4: Corrosion rates and mass loss rates calculated for unirradiated Zy-4 samples.

Samples	**Corrosion rate nm/y**	**MR μg/ cm^2 y**
as received Zy-4 aerobic cond	480	310
as received Zy-4 anaerobic cond	110	75
Zy-4 oxidised aerobic cond.	9.72	6.58
Zy-4 oxidised anaerobic cond	3.16	2
Zy-4 oxidised, cut aerobic cond	11.6	7.5

5 Work in progress at JRC-ITU

5.1 *Cleaning procedures*

- Irradiated samples containing fuel will be cleaned with either 7M HNO_3 or (more likely) 15% H_2SO_4, as it is performed by INE. Then, the samples will be rinsed with water.
- Irradiated samples from the plenum (ie. not containing fuel but with fission product deposits) will be cleaned with either 1M HNO_3 or dilute H_2SO_4. Then, they will be rinsed with water.
- Non-irradiated samples will be cleaned with alcohol and then rinsed with water and dried out.

5.2 *Leaching test*

ITU has worked on the experimental setup regarding the leaching experiment in the autoclave. The sample will be Zircaloy-4 with a thin outer liner Zr-2.5Nb. Non-irradiated samples of 15-15-Ti and Zircaloy -4 are available for comparison.

To determine the leach (or corrosion) rates, ITU will use Co-60 (gamma-spec). Gravimetric measurements are considered not appropriate for Zircaloy in cementitious medium as the expected corrosion rates are too low to be determined accurately.

Zircaloy samples will be tested in a solution of NaOH at pH 12.5 at two different temperatures: T 30°C and 80°C. The autoclave testing will be done at slightly above atmospheric pressure (e.g. 1.5 bar) to enable easier gaseous sampling.

Non-irradiated samples of the cladding material will be analysed and metallography characterisation will be conducted by using optical microscopy as well as scanning electron microscopy coupled with energy dispersive X-ray spectroscopy (SEM/EDS).

References

ASTM (2013). ASTM E112-13 Standard test method for determining average grain size.

HERM, M, GONZÁLEZ-ROBLES, E, BÖTTLE, M, MÜLLER, N, PAPAIOANNOU, D., WEGEN, D H, DAGAN, R, KIENZLER, B, METZ, V. 2015. Description of Zircaloy-4 dissolution experiment in a shielded box (CAST project Deliverable 3.8)

KATO, O, TANABE, H, SAKURAGI, T, NISHIMURA, T, TATEISHI, T. 2014. Corrosion tests of Zircaloy hull waste to confirm applicability of corrosion model and to evaluate influence factors on corrosion rate under geological disposal conditions, In: *Materials Research Society Proceedings,* Vol. 1665, 195-202.

KEN'ICHI ITO, KATSUMASA HAIKAWA, ET AL. (1998). Top Technologies of ABWR Part 2: BWR CORE AND FUEL TECHNOLOGIES. 47.

S.NECIB, D. BOTTOMLEY, ET AL. (2014). Annual WP3 progress report, Deliverable D3.5, CAST PROJECT.

SAKURAGI, T, MIYAKAWA, H, NISHIMURA, T, TATEISHI, T. 2013. Long-term corrosion of Zircaloy-4 and Zircaloy-2 by continuous hydrogen measurement under repository condition, In: *Materials Research Society Proceedings,* Vol. 1518, 173-178.

VAN RENTERGHEM, W. 2015. Microstructure of the RPV-steel and Zircaloy 4 used in the project CAST. Internal SCK•CEN report. Belgian Nuclear Research Centre.

YAMAGUCHI, T, TANUMA, S, YASUTOMI, I, NAKAYAMA, T, TANABE, H, KATSURAI, K, KAWAMURA, W, MAEDA, K, KITAO, H and SAIGUSA, M. 1999. A Study on Chemical Forms and Migration Behavious of Radionuclides in Hull Wastes. Radioactive Waste Management and Environmental Remediation, *Proceedings of the ASME 1999 ICEM conference,* September 26-30, Nagoya, Japan, ASME.

YAMASHITA, Y, TANABE, H, SAKURAGI, T, TAKAHASHI, Y, SASOH, M. 2014. C-14 release behavior and chemical species from irradiated hull waste under geological disposal conditions, In: *Materials Research Society Proceedings*, Vol. 1665, 187-194.